JOURNAL OF MATERIALS SCIENCE 29 (1994) 424–435

Nucleation mechanism of the cubic σ phase in squeeze-cast aluminium matrix composites

R. D. SCHUELLER*, F. E. WAWNER
Department of Materials Science and Engineering, University of Virginia, Charlottesville, VA 22903, USA

A. K. SACHDEV
Metallurgy Department, GM Research Labs, Warren, MI 48090, USA

An Al–4.3 wt% Cu–2.0 wt% Mg alloy reinforced with 20 vol% reinforcing fibres was examined after a T7 heat treatment. The expected precipitate phase was equilibrium S′ (Al_2CuMg), which was confirmed to form in the monolithic alloy. However when this Al–Cu–Mg alloy was squeeze-cast into a fibre preform and given an identical T7 heat treatment a number of other phases also nucleated; these included θ′ (Al_2Cu), β′ (Mg_2Si) and the cubic σ phase ($Al_5Cu_6Mg_2$). These additional phases were determined to nucleate and grow rapidly during the water-quench following solution treatment. The existence of excess Si (approximately 0.5 wt%) in the matrix was determined to be responsible for nucleation of these additional phases. This extra Si entered the composite matrix during squeeze-casting through breakdown of an SiO_2 layer which existed at the fibre interfaces. During quenching Si clusters rapidly form and provide nucleation sites for the σ and θ′ phases. The Si clusters apparently created a compressive strain in the matrix which attracted a high concentration of small Cu atoms to their interface. The σ phase nucleated in this high-Cu region since, on a localized scale, σ became the equilibrium phase. This type of nucleation process may also explain the enhanced precipitate nucleation which occasionally takes place in other alloy systems when trace amounts of certain elements are added.

1. Introduction

This paper will address the nucleation mechanism responsible for formation of the metastable σ phase in squeeze-cast Al–Cu–Mg alloy composites. The cubic-shaped σ phase has been identified in a previous paper as $Al_5Cu_6Mg_2$ [1]. These precipitates were generally found in sizes ranging from 30 to 50 nm and existed in volume fractions as high as 3.8%. The σ phase has been shown to have good potential for precipitate strengthening, but more importantly it appears to be coarsening-resistant up to temperatures as high as 250 °C [2]. Therefore this phase could conceivably extend the useful temperature range of aluminium alloys and aluminium-matrix composites, thus making them suitable for elevated-temperature aerospace applications.

In order to obtain the maximum increase in yield strength from the σ phase a homogeneous distribution of small 2.7 nm cubes is required [2]. This microstructure, however, has not yet been achieved in practice. To attain this goal a much larger number of nucleation events is necessary. Past investigations have shown the cubic σ phase to only nucleate in Al–Cu–Mg alloys after the addition of a small amount of Si [3–5]. To increase the nucleation rate of σ in the aluminium alloy a better understanding must be gained as to how Si influences its nucleation.

The mechanism by which Si nucleates the σ phase is also important since it could shed light on how additions of certain trace elements to aluminium alloys can increase the nucleation rate of precipitates in the alloy. For example, additions of Cd, In, or Sn to Al–Cu alloys has been shown to increase the nucleation rate of θ′ directly from the matrix [6–10]. The addition of Ag to Al–Cu–Mg alloys results in increased nucleation of Ω phase [11]. Furthermore, the addition of Zn and Mg to an Al–Zr alloy induces nucleation of Al_3Zr, as does the addition of Si alone [12]. The mechanism by which these additions induce precipitate nucleation is unknown.

1.1. Squeeze-casting

One of the primary reasons metal-matrix composites have gained increased attention in recent years is due to the development of more economically attractive fabrication techniques such as squeeze-casting. Squeeze-casting offers good microstructural control at relatively low cost. With this technique composite parts can be cast directly into their final net shape, eliminating waste material. Squeeze-casting also allows selective reinforcement of only the areas of the casting which would benefit from the composite properties. The pressure applied during casting can

*Present address: Electronic Products Division, 3M Center, Austin, TX 78769, USA.

0022–2461

also aid in wetting the reinforcement and helps to prevent porosity and shrinkage.

2. Experimental procedure

2.1. Materials

The squeeze-castings fabricated for this study were made by forcing superheated molten aluminium (at 700–800 °C) into a porous preform under high pressure (up to 20 MPa). The preform was a disc-shaped network of fibre reinforcement 9 cm in diameter and 1.5 cm thick which contained 20 vol % reinforcement. Prior to infiltration, the preform was heated in air to temperatures in excess of 800 °C to ensure that the aluminium did not solidify upon contact with the whiskers.

A number of Al–Cu–Mg alloys with varying composition were squeeze-cast into SiC preforms. The primary matrix composition used was Al–4.3Cu–2Mg. However, alloys with Al–4.3Cu–3Mg and Al–4.3Cu–4Mg reinforced with SiC whiskers were also examined. In addition to SiC whiskers, two other types of reinforcement were studied with the Al–4.3Cu–2Mg matrix. These included crystalline aluminium oxide, Al_2O_3, (Saffil) and aluminosilicate (Kaowool), which is a nearly even mixture of Al_2O_3 and SiO_2. The Saffil fibres contained a 3% silicon addition to improve their properties.

Eventually alloys with Si added to them (Al–4.3Cu–2Mg–0.35Si and Al–4.3Cu–2Mg–0.8Si) were squeeze-cast into SiC preforms. Unreinforced alloys of Al–4.3Cu–2Mg and Al–4.3Cu–2Mg–0.3Si were also examined. The initial material examined was given a T7 heat treatment at General Motors Corp., which included a 16 h solution treatment at 529 °C followed by a quench into 65 °C water and 5 h artificial ageing at 190 °C.

Various heat treatments were also performed at the University of Virginia. Most samples were wrapped tightly in two layers of aluminium foil and solutionized in a salt bath at 530 °C. These samples were generally quenched in an ice brine, except where noted. Ageing treatments were performed in a salt bath. For a more rapid quench thin samples (0.3–0.5 mm thick) were solutionized in a wire basket and either quenched in ice brine or quenched directly to the desired ageing temperature in a salt bath.

3. Results

3.1. Microstructural observations

Studies have previously shown that aluminium alloys with a Cu:Mg ratio between 4:1 and 1.5:5 would be expected to contain exclusively equilibrium S′ (Al_2CuMg) after quenching and ageing [13–15]. Wilson [16], among others, revealed that vacancy loops rapidly form in these alloys upon quenching from solution temperature. The S′ needles preferentially nucleate on these defects. This phenomenon was expected in the Al–4.3Cu–2Mg composite matrix (a Cu:Mg ratio of 2.15:1) and was confirmed in the unreinforced portions of the castings which were given a T7 heat treatment (Fig. 1).

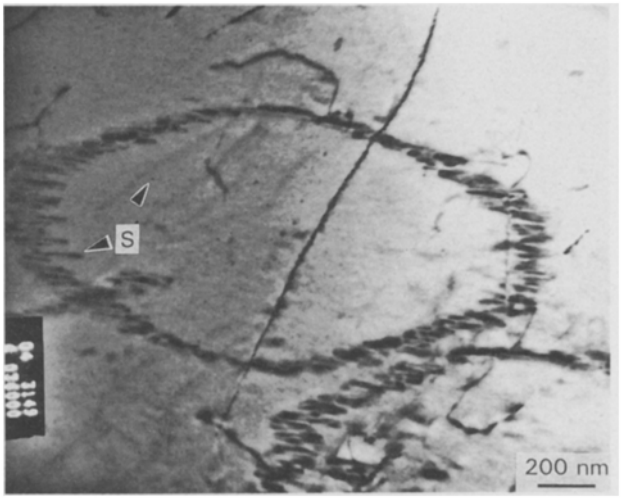

Figure 1 Unreinforced Al–4.3Cu–2Mg, T7. Vacancy loops with S′ nucleating on them. Smaller S′ had nucleated between loops.

However, the precipitate microstructure in the reinforced section of the squeeze-castings (also given a T7 heat treatment), was surprisingly different (Fig. 2). Vacancy loops no longer formed to provide heterogeneous nucleation sites for S′. Although S′ did form in the matrix, it made up a much lower volume fraction than in the monolithic alloy. The plate-shaped θ′ phase (Al_2Cu) also nucleated in the matrix. This phase is common to Al–Cu alloys and is not typically observed in alloys with such a low Cu:Mg ratio. In some instances the rod-shaped β′ phase (Mg_2Si) was also detected. Of most interest, however, was the unusual cubic-shaped σ phase. This phase had rarely been observed in the past and had never been identified or examined in detail. The σ phases were only observed in scattered regions of the bulk sample, thus only a small fraction of TEM samples contained them. However, in some foils the cubes were densely distributed in volume fractions as high as 3.8%.

Squeeze-cast composites were also fabricated with Kaowool and Saffil fibres and given a T7 heat treatment. The σ phase nucleated in these composites as well. In addition, SiC preforms were infiltrated with alloys containing higher concentrations of Mg (Al–4.3Cu–3Mg, Al–4.3Cu–4Mg). The cubic σ phase was also detected in these higher Mg containing matrices, although in these the θ′ phase was less abundant than in the 2Mg matrix.

3.2. Precipitate nucleation

To determine at what point during the T7 heat treatment the assorted phases nucleated, samples of the SiC reinforced composite (1 cm × 1 cm × 5 cm) were examined after being exposed to various stages of the T7 heat treatment. For example, as-cast, aged only, solutionized and quenched only, and solutionized, quenched and aged materials were examined. A high concentration of σ and θ′ (and also some β′) were observed in the sample which had been solutionized and warm water-quenched only; however, no S′ was present in this sample (Fig. 3). A few cubic σ phases

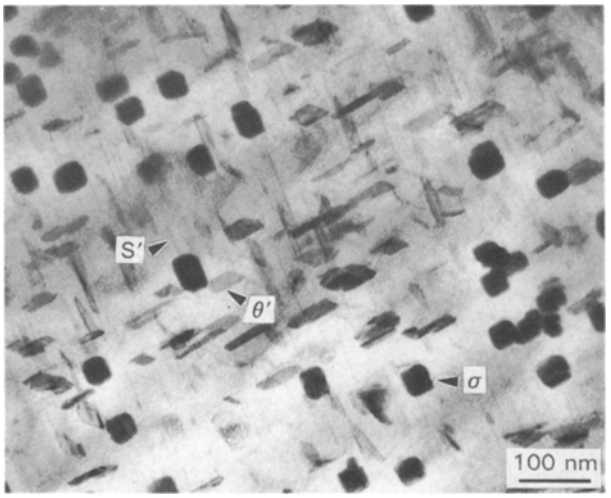

Figure 2 Al–4.3Cu–2Mg reinforced with 20 vol % SiC whiskers, T7. S', θ' and cubic σ phases are shown.

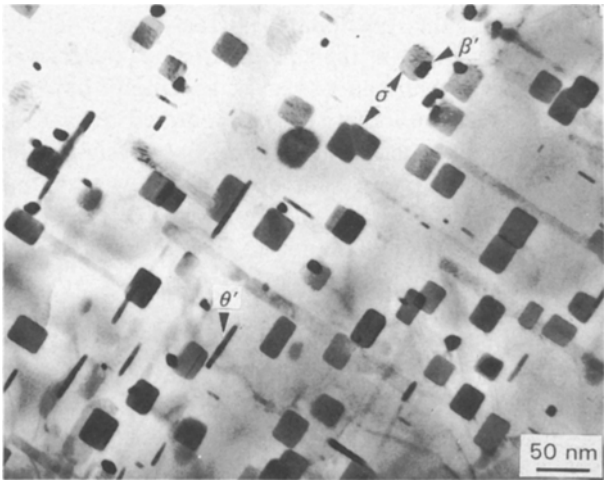

Figure 3 Al–4.3Cu–2Mg–0.35 Si/SiC composite solutionized and quenched in warm water. σ, θ' and β' formed during this quench. No S' nucleated.

were also detected in an as-cast sample. These observations suggested that σ, θ' and β' nucleated and grew during the quench into warm water and not during ageing at 190 °C, as was originally believed. Thin samples (2 mm thick) quenched even more rapidly in ice brine also contained the σ, θ' and β' phases. These results were quite surprising, since similar cooling rates in the unreinforced alloy resulted in no detectable precipitation.

Samples air-cooled after solution treatment (at an average cooling rate of 8 °C $^{-1}$) also contained σ, θ' and β' phases. Once again, S' was not present in these cooled samples. The S' phase only appeared to nucleate during subsequent ageing conditions, implying it has a slower nucleation rate than the other phases in this alloy. Samples cooled very slowly (furnace-cooled) contained large θ', β' and S' phases. These probably formed at very high temperatures during cooling.

3.3. The source of excess Si in the composite

Using energy-dispersive X-ray spectroscopy (EDXS) techniques, elemental Si was detected in the composite matrix in local concentrations up to 1 wt %; however, in most areas the concentration was roughly about half this value. Although Si concentrations less than 1 wt % could not be determined accurately with the EDXS system (due to the close proximity of the Al and Si K_α peaks), it was obvious that the amount of Si in the matrix was much higher than in the precast alloy (0.06 wt %). The existence of β' (Mg_2Si) rods in the matrix also indicated the presence of excess Si. Consequently, this Si must have entered the matrix during fabrication of the composite. Since previous investigations have shown the cubic phase to only form in Al–Cu–Mg alloys after the addition of small amounts of Si (0.2–0.5 wt %) [3–5], this excess Si is clearly responsible for the formation of the σ phase in the composite matrix. To further verify this effect of Si, a small amount of Si (0.35 wt %) was added to the monolithic Al–4.3Cu–2Mg alloy. The σ phase was confirmed to nucleate in this monolithic alloy.

The excess Si in the composite matrix was determined to originate from breakdown of silica (SiO_2) present in the reinforcing preform. The fibres in the preform are frequently held together with a silica binder which is applied to the surface of the fibres. In addition, before the squeeze-casting fabrication process takes place, the reinforcing preform is heated in air to temperatures near 800 °C. Previous studies have revealed that an SiO_2 layer quickly forms at the surface of SiC whiskers when they are exposed to elevated temperatures [17–19]. For example, the rapid growth of a 25 nm thick silica layer was clearly shown in a study by Marr and Ko [18] using SiC fibres heated in air for 1 h at 600 °C. These results agreed with observations by Henriksen [17] who reported a 20 nm layer of silica at the surfaces of whiskers heated as a preform to 800 °C prior to squeeze-casting.

The Mg in the superheated molten aluminium apparently reacted with the SiO_2 during fabrication through one or both of the following reactions:

$$SiO_2 + 2Mg \Rightarrow 2MgO + Si \quad (1)$$

$$2SiO_2 + 2Al + Mg \Rightarrow MgAl_2O_4 + 2Si \quad (2)$$

Li *et al.* [20] observed MgO at whisker interfaces in their squeeze-cast composite and suggested that Reaction 1 was taking place. Henriksen [17] on the other hand reported the presence of $MgAl_2O_4$ (spinel) at the interface of SiC fibres and proposed Reaction 2 for the breakdown of SiO_2. A study by Munitz *et al.* [21] discovered that the Si present in Saffil fibres (recall that the Saffil fibres contain 3% Si to enhance properties) was also reduced during processing, which resulted in formation of both spinel and MgO at the interface. Similar results were also noted by Levi *et al.* [22]. In the formation of MgO and $MgAl_2O_4$ free Si is a product of the interfacial reaction and is therefore allowed to diffuse into the molten metal.

Mg-containing oxides were indeed observed at the whisker interfaces in the composites studied (Fig. 4), suggesting that these reactions were taking place. However, it is unclear whether the interfacial oxide is MgO or spinel. Additional evidence of Mg reacting

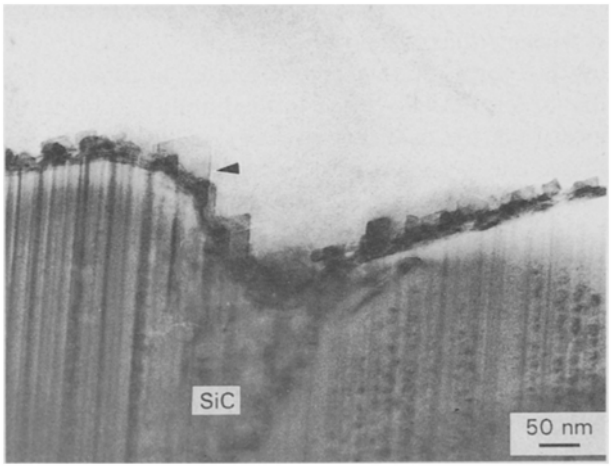

Figure 4 Mg-containing oxide at the interface of an SiC whisker.

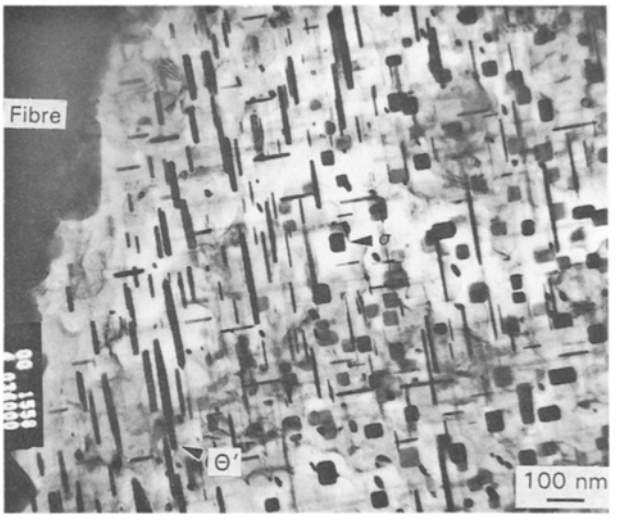

Figure 5 A region depleted of Mg near a Kaowool whisker. θ′ is dominant in this region since the σ phase cannot form.

with the SiO_2 at the interfaces of whiskers can be seen in Fig. 5. This micrograph shows a Kaowool fibre with thick Mg-containing oxides at the interface. An Mg-free region (0.7 μm wide) existed near the interface. In this region few Mg-containing phases were able to nucleate (including σ), so only θ′ is present. The interfacial reaction apparently depleted the nearby matrix of Mg.

Calculations reveal that if a 25 nm layer of SiO_2 (on typical-sized whiskers 5 μm in length and 0.7 μm in diameter, which make up 20 vol % of the composite) were broken down by Mg, 0.49 at % Si would be released into the matrix. This amount is sufficient to cause nucleation of the σ phase and is in agreement with observations. The presence of Mg-containing oxides at the interface of SiC, Kaowool and Saffil fibres implied that SiO_2 was being broken down at the interface of all these fibres, thus explaining why the σ phase was observed in the matrix of all three composite systems

It is likely that the interfacial breakdown of SiO_2 took place during the high 700 °C fabrication temperature rather than during solutionizing at 530 °C. The presence of the σ phase in regions of the as-cast, unheat-treated material supports this view.With this method of Si entry, the local concentration of Si depended on a variety of factors, including: (i) the number of whiskers nearby, (ii) the thickness of the SiO_2 layer on the nearby whiskers, (iii) the local concentration of Mg available for breakdown of the silica layer, and (iv) the total time the superheated molten aluminium is in contact with the whiskers. These variables resulted in an unreliable concentration and uneven distribution of Si in the composite matrix. In an attempt to obtain a more even distribution of Si, and thus a more consistent microstructure, some castings were fabricated using an aluminium alloy in which small amounts of Si (0.35–0.85 wt %) were directly added. Although the σ phase did indeed nucleate more consistently in these composite matrices, the results were still unsatisfactory due to the tendency of Si to segregate. That is, while some regions had the correct concentration of Si to nucleate σ other regions did not.

3.4. Reproducing the cubic σ phase

For the σ phase to be of any practical use, a reliable method of forming this phase in a consistent manner throughout a bulk sample must be developed. It is obvious that in order to get a significant concentration of fine σ phase a high nucleation rate is required. It was shown that the σ, θ′, and β′ phases formed in the composite during air cooling, warm water quenching and ice brine quenching. However, nucleating the σ phase through controlled cooling of the material may not be the most reliable or optimum method of obtaining the maximum number of nucleation events. Therefore other heat treatment methods were also investigated.

The most success was achieved by quenching samples in a salt bath directly to various temperatures in order to determine the temperature at which the σ phase nucleated. Then perhaps the material could be held at this temperature for a longer period of time to allow more nucleation events to occur. In 2 mm thick samples quenched directly to temperatures ranging from 240 to 340 °C and aged for 10 min, the microstructure generally consisted of large θ′ phases with fine θ′ and σ between them. Apparently the quench was not rapid enough to prevent formation of the large θ′ phases at high temperatures (> 350 °C). The finer θ′ and σ phases formed during ageing in the 240–340 °C range. Thin samples (< 0.5 mm) quenched directly to these temperatures contained fewer large θ′ phases and a more even distribution of fine θ′ and σ. However, there were still many samples which did not contain any precipitates at all. Since EDXS revealed a sufficient concentration of Cu and Mg in solution in these precipitate free regions, these regions were probably devoid of precipitation due to the segregation effects of Si. The segregation problems associated with Si are well known and difficult to overcome. The inconsistent nucleation of the σ phase made it impossible to determine more accurately the optimum temperature for σ phase nucleation.

The largest remaining obstacle preventing controlled formation of the σ phase appears to be the

segregating characteristics of Si. The best method of obtaining a sufficiently high rate of σ phase nucleation throughout an alloy may be by discovering another element which also causes nucleation of the σ phase but does not have the segregation problems associated with Si. To find such an element, a better understanding is required of how Si caused nucleation of σ.

4. Discussion

4.1. Nucleation of σ phase from Si clusters

It was shown earlier that the equilibrium precipitate phase in an Al–4.3Cu–2Mg alloy is S′. However, when small amounts of Si (0.2–0.5 wt %) were added to this alloy other precipitates (including σ and θ′) were observed to nucleate. The nucleation mechanism of the σ phase will be discussed first.

According to the ternary Al–Cu–Mg phase diagram, the σ phase is only in equilibrium at compositions near 60 wt % Cu and 2–10 wt % Mg (Fig. 6) [23]. In fact Mondolfo [24] has stated that the $Al_5Cu_6Mg_2$ phase is not in equilibrium in any aluminium-rich alloy. Therefore, it is unlikely that the addition of a small amount of Si to the system would radically alter the phase diagram to the point where σ was the lowest energy precipitate. Consequently, the σ phase must be a metastable phase which was allowed to nucleate due to the presence of Si.

It is known that metastable phases, in general, are able to form in alloys due to their ability to nucleate faster than the more energetically stable equilibrium phase. This was shown to be the case in this system where σ and θ′ nucleated during the quench whereas S′ only nucleated during subsequent ageing. Therefore the excess Si must increase the nucleation rate of the σ and θ′ phases relative to the S′ phase. Metastable phases are often able to nucleate more rapidly than those in equilibrium due to lower values of surface energy, γ, and/or volume strain energy, ω. These terms reduce the nucleation energy barrier, ΔG^*, which is written as [25]

$$\Delta G^* = A^*\gamma + V^*(g_v + \omega) \quad (1)$$

where: γ is the surface energy of the embryo, ω is the misfit strain energy per volume of the embryo, g_V is the volume free energy of the phase (or the driving force for nucleation, a negative value), A^* is the surface area of a critical-size embryo and V^* is the volume of a critical-size embryo.

Since the actual nucleation of the σ phase occurs on a very small scale and at a rapid rate, the nucleation process could not be observed directly. Intuitive

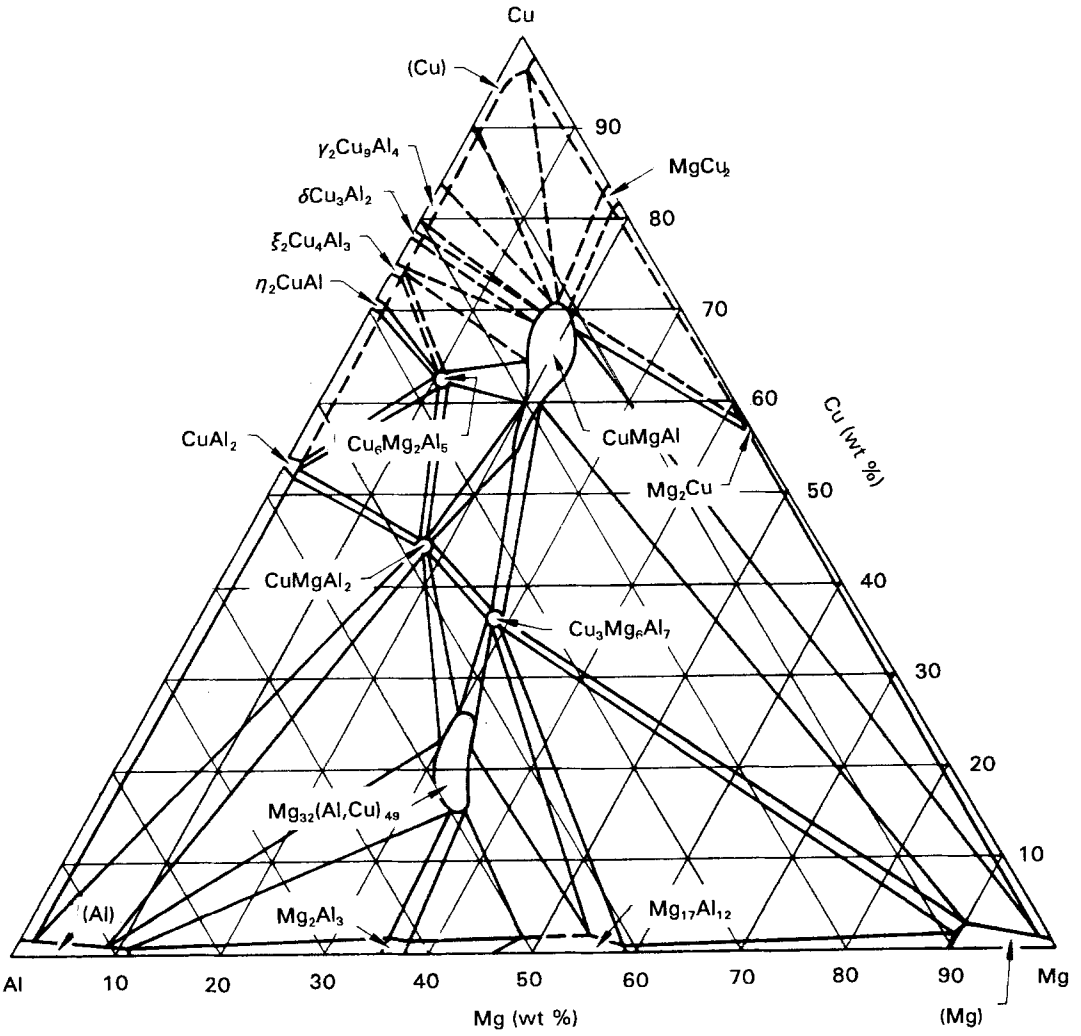

Figure 6 Equilibrium ternary Al–Cu–Mg phase diagram at a 400 °C isotherm [23].

reasoning was instead used to determine the method by which this phase nucleates. The following statements about the σ phase and the alloy system are factors which need to be considered:

1. Past studies have shown the cubic σ phase to only form in Al–Cu–Mg alloys after the addition of a small amount of Si (0.2–0.5%).
2. The σ phase itself contains no Si.
3. The Si must therefore be responsible for the rapid nucleation of the σ phase.
4. The complex structure (39 atoms per cell) and large lattice constant ($a = 0.831$ nm) suggests the σ phase cannot nucleate homogeneously within the matrix.
5. Since this phase consists of 46 at % Cu, a high concentration of Cu is required on a local scale for this phase to nucleate.
6. The σ phase nucleates and grows rapidly during the warm water quench following solution treatment.

Another point to consider is the behaviour of Si in aluminium alloys. For example, many studies have been performed to determine the Si–vacancy binding energy in aluminium. These studies generally report a higher value of binding energy for Si (From 0.20 to 0.23 eV [26, 27]) than for Mg (0.18 eV [28, 29]) or Cu (0.05 eV [28]). More recent studies often give much smaller values for these binding energies due to a more accurate value of vacancy formation energy (for example Takamura *et al.* [30] reports an Si binding energy of 0.07 eV). However, the binding energy of Si would still be expected to be greater than that of Mg or Cu. Two effects of vacancies being bound to Si are (i) the diffusion of Si is very rapid in aluminium after quenching (since there is usually a vacancy nearby for the Si atom to jump into), and (ii) vacancies are prevented from going to vacancy sinks, such as vacancy loops, upon quenching.

Another interesting property of Si in aluminium is its rapid decrease in solubility as the temperature is reduced from solution, as shown in Fig. 7. For instance at 529 °C up to 1.05 at % Si can be dissolved into solution; however, when cooled to 280 °C a maximum of only 0.04 at % Si is in solution [31]. Thus, upon quenching, there is a large force driving the Si out of solution. The combined effects of this force and the high diffusivity of Si (as mentioned above) results in the rapid formation of Si clusters as the alloy is cooled from solution temperature, as previously shown by Rack and Krenzer [32] and Rosenbaum and Turnbull [33]. Very small (1–3 nm) coherent Si clusters have been determined to quickly form in these alloys through resistivity measurements and TEM [34]. In fact it was demonstrated by Kovaks *et al.* [35] that precipitation in any aluminium alloy containing Si always began with the clustering of Si atoms. In these clusters Si has an atomic volume of 0.0200 nm^3 per atom which is 21% larger than that of the aluminium matrix (in which the atomic volume is 0.0165 nm^3 per atom, see Table I). Thus, a spherical cluster 3.0 nm in diameter, for example, would essentially be forced into a void with a diameter of 2.8 nm and a compressive volume strain is created in the matrix. In an alloy with 0.5 at % Si these 3 nm clusters would be spaced a distance of 13 nm apart. Therefore, the strains between clusters could reach nearly 1.5%.

It is therefore proposed that as the material is quenched these Si clusters rapidly form, creating compressional strains in the surrounding aluminium matrix. Many of the vacancies which transported the Si atoms to the cluster would remain near the cluster to help relieve this strain, as demonstrated earlier by Rosenbaum and Turnbull [33]. This phenomenon had also previously been shown to occur in copper alloys in which silica and alumina are internally oxidized [36]. When these oxides formed they created a compressive strain on the copper matrix which was then relieved by vacancies. If the alloy in the present investigation contained 0.5 at % Si, calculations show that the vacancies available after a solution treatment at 530 °C (0.0088 at %) would not be plentiful enough to relieve all the strain created by the Si clusters within the matrix. In fact, only 4% of the strain could be relieved by the available vacancies. As a result, one would expect that the relatively small Cu atoms (with an atomic volume of 0.0118 nm^3 per atom) would be attracted to the cluster–matrix interface to relieve the remaining strain and thus lower the energy of the system, as illustrated in Fig. 8. There is plenty of Cu available for this purpose since only 0.4 at % Cu is required to relieve all the strain caused by the clusters. This mechanism is similar to the way in which Cu atoms are attracted to the compressive side of an edge dislocation where θ′ is then known to nucleate.

This same mechanism is also consistent with the results of Stewart and Martin [37] who demonstrated that adding Cu to an Al–Si alloy increased the nucleation rate of Si precipitates and allowed them to form into equiaxed spheres as opposed to the plates and rods which form in binary Al–Si alloys. The Cu

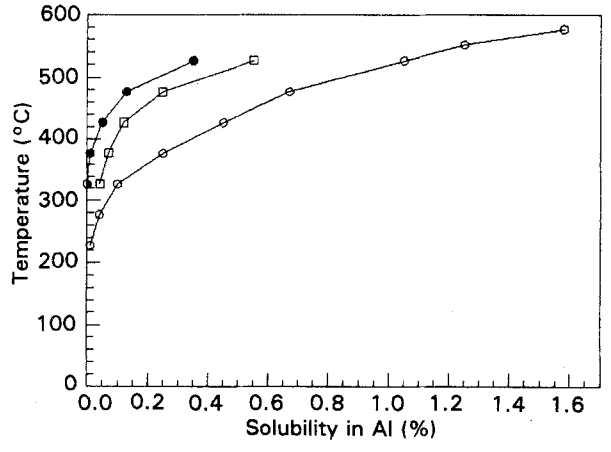

Figure 7 Solubility in aluminium of (○) Si and of Mg_2Si with an excess of (□) 1% and (●) 1.5% Mg over the Mg_2Si composition [31, 45].

TABLE I Atomic volume associated with phases and elements (10^{-30} m^3/atom)

Al	θ′	σ	S′	β	Si	Cu	Cd	Sn	In
16.5	15.8	14.7	16.6	21.0	20.0	11.8	21.6	27.0	26.1

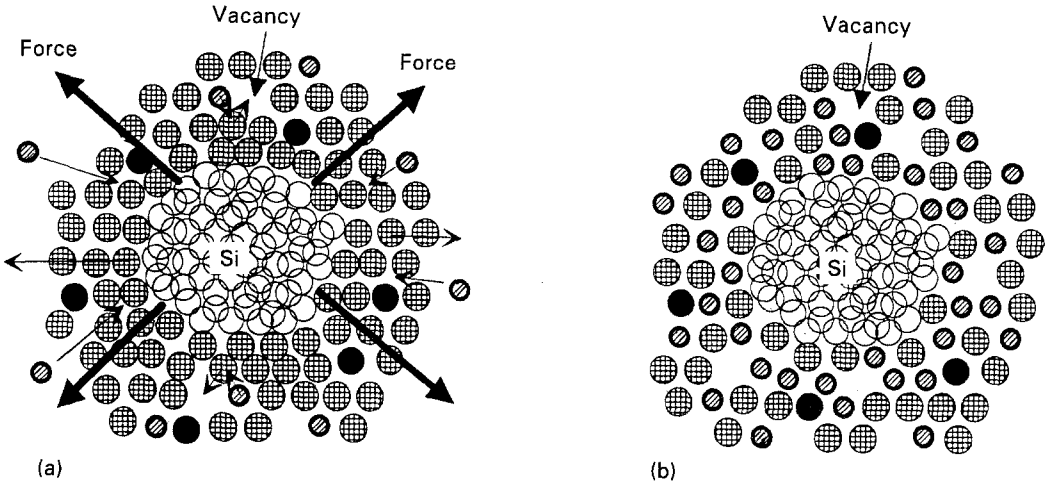

Figure 8 Proposed nucleation mechanism of the σ phase. (a) Immediately following Si cluster formation. An Si cluster exerts a compressive stress on the aluminium matrix. (b) A short time later. Vacancies and smaller Cu atoms diffuse to the region surrounding the cluster where they relieve the compressive stress. (●) Al, (▨) Cu, (●) Mg.

apparently increased the nucleation rate of Si by relieving the volume strain created by the Si cluster. This relief of strain also allowed the phase to grow in all directions, resulting in the equiaxed structure. A small addition of Cu to an Al–Mg–Si alloy has also been shown to increase the nucleation rate of Mg_2Si [38] (Mg_2Si also has a large atomic volume associated with it, as seen from β in Table I). Furthermore, it has been shown that the presence of Cu reduces the solubility of Mg_2Si in aluminium; that is, Mg_2Si precipitates out at a higher temperature [39]. This phenomenon can also be explained by the interaction of Cu with the strain field. Finally, Chatterjee and Entwistle [40] demonstrated that an addition of Cu decreased the resistivity of an Al–Mg–Si alloy upon ageing. The authors attributed this effect to a slowing down of Mg_2Si nucleation; however this effect can just as easily be explained by a reduction in the strain field around the Mg_2Si phase by the Cu. After all, it is the strain field caused by the Mg_2Si precipitation which is responsible for the rise in resistivity in the first place [41].

In the Al–Cu–Mg–Si alloy, the Cu-rich region near the Si cluster would, therefore, become an ideal location in which the σ phase could nucleate. The concentration of Cu near the cluster could reach values high enough so that locally the alloy is near that in which the $Al_5Cu_6Mg_2$ phase is the low-energy phase, i.e. near 50–60 wt % Cu and 2 wt % Mg (note that the required Mg composition is already satisfied by the matrix). Also, the relatively high concentration of vacancies in this region would allow rapid mixing of the atoms (the jump rate of a vacancy at 200 °C, for example, is approximately $10^7\ s^{-1}$ [42]), making rapid nucleation of the complex σ phase more likely. Furthermore, since the atomic volume in the σ phase is 11% less than that in aluminium, the compressed region near the cluster would favour σ phase nucleation. In this region the volume strain term, ω, would be much smaller than if the σ phase nucleated in the aluminium matrix away from the cluster, so the energy barrier for nucleation is reduced.

In addition to Si providing a nucleation site for σ, it also aids the nucleation of this phase by slowing down nucleation of the equilibrium S′ phase. It was noted that with the addition of Si, vacancy loops no longer formed in the alloy. These vacancy loops provided a heterogeneous site for rapid S′ nucleation. Without these nucleation sites the S′ must instead nucleate from GPB in the matrix, which is a much slower process.

4.2. Nucleation of the σ phase from Mg–Si clusters

It is also possible that Mg–Si clusters quickly form in the composite matrix upon quenching and nucleate the σ phase in a manner similar to that just described for Si clusters. After all, it is well known that the binding energy between Mg and Si is very high (the enthalpy of formation is − 26.8 kJ per g-atom and the melting temperature is 1085 °C [43]) and that Mg–Si clusters rapidly form in Al–Mg–Si alloys during quenching [44]. In addition, it has been shown that the greater the excess of Mg above the Mg_2Si composition the lower the solubility of the Mg_2Si phase, as was seen in Fig. 7 [45]. Thus when small amounts of Si (for example 0.5 at %) are added to the alloy with 2 at % Mg, the 1 at % excess Mg would cause Mg_2Si to precipitate out at high temperature. Also, as mentioned earlier, Cu can further decrease the solubility of Mg_2Si, thus further aiding rapid formation of Mg–Si clusters in the Al–Cu–Mg–Si system.

The atomic volume in these clusters is estimated as 0.021 nm^3 per atom (if the equilibrium β structure is assumed, as shown in Table I) implying that these Mg–Si clusters would also create a volume strain in the matrix. This agrees with past studies which have shown these clusters to be rich in vacancies [44, 46]. In fact Mg–Si clusters have been known to nucleate the θ′ phase in Al–Cu alloys as shown by Brook and Hatt [46].

In spite of the strain created by the cluster, it is believed that if plenty of Si and Mg were available the

very stable β′ phase would rapidly grow from the cluster, as was the case in samples containing a high concentration of Si. However, if a smaller concentration of Si were available (0.3–0.5 at %), growth of the cluster would be stunted, thus allowing Cu atoms to diffuse to the interface to relieve the strain and nucleate the σ phase. It should also be noted that if only trace amounts of Si (< 0.3 at %) were available, the very small clusters which form would not likely be large enough to create the necessary volume strains required for nucleation of the σ phase.

4.3. Detection of Si or Mg_2Si clusters

The projected small size (< 3 nm) of the Si or Mg_2Si clusters made them difficult to detect with the TEM, primarily because they were not thick enough to cause a significant contrast variation and because the elements of Al, Mg and Si have similar scattering factors [48] due to their closeness in the periodic table. However, even though the clusters themselves are too small to be seen, the volume strain created by them should theoretically be detectable. The bending of the aluminium planes around the cluster should create contrast effects similar to the way in which dislocations do.

According to past studies [49, 50], the symmetrical strain created by a spherical cluster which compresses the surrounding matrix would appear under a two-beam condition as a pair of lobes with a line of no contrast between them (where the line of no contrast is perpendicular to the operating reflection). This lobed contrast phenomenon, which apparently resulted from Si or Mg–Si clusters, was occasionally observed in the composite matrix; an example can be seen in the micrograph in Fig. 9. The strain field around the clusters has a diameter of approximately 3.5 nm, so the cluster itself is probably 2–3 nm in diameter. The closeness of the Si, Al and Mg X-ray peaks made it impossible to determine whether the clusters were pure Si or Mg_2Si.

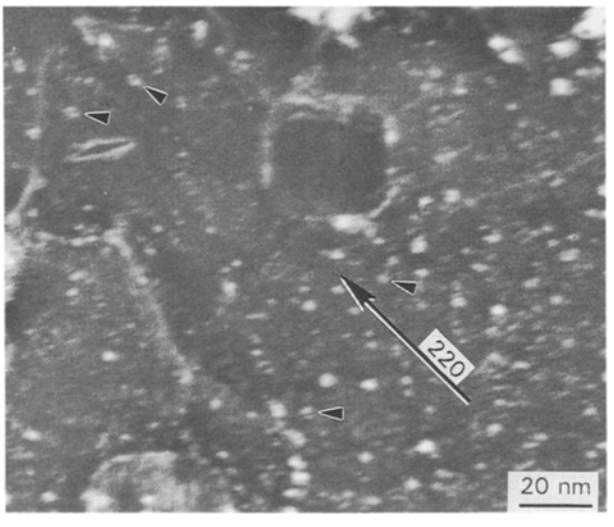

Figure 9 Lobed contrast possibly resulting from symmetrical strain field surrounding a small (< 3 nm) cluster.

This lobed contrast effect, however, was not observed in all the samples examined, possibly due to the small size and long exposure times required to image them in weak beam, dark field conditions. It is also possible that the compressive strain created by the clusters is rapidly relieved by the Cu atoms and vacancies which diffuse to the interfacial region. A previous investigation by Ashby and Smith [36] supports this argument. These authors demonstrated that when a particle with a larger atomic volume than the surrounding matrix grew, the compressive strain created in the matrix was quickly relieved by vacancies which diffused to the interfacial region, i.e. the strain annealed out as rapidly as it formed. Therefore the particles in Ashby and Smith's investigation did not exhibit the lobed strain field that was expected.

The presence or identity of the small clusters could not be confirmed with diffraction techniques due to the low volume fraction of these clusters. For instance, if Si clusters formed in an alloy with 0.5 wt % Si, these clusters would constitute a maximum volume fraction of only 0.6%. Therefore any diffraction effects would be minute, or even undetectable. In addition, these clusters may be randomly oriented in the matrix, thus further reducing any diffraction effects.

4.4. Growth of the σ phase

The fact that the σ phase nucleated and grew to sizes as large as 50 nm during a rapid ice water quench was quite surprising. In the Al–4.3Cu–2Mg alloy, growth of the σ phase to 50 nm would require depletion of Cu from a cubic volume with an edge length of 150 nm in a period of less than 1 s. It was shown earlier that the σ phase nucleated at temperatures near 300 °C during cooling. At this temperature the time required for the growth of the precipitate by simple diffusion of Cu through the lattice was calculated to be 65 s (this is the time required for a Cu atom to diffuse through the lattice from the outer edge of the Cu-depleted region to outer edge of the precipitate using a D_0 of 0.647 $cm^2\ s^{-1}$, a Q of 135 $kJ\ mol^{-1}$ [51], and a random atom jump distance of $d = (Dt)^{1/2}$). This estimated time for growth by lattice diffusion is actually a lower bound since all the surrounding Cu atoms were assumed to diffuse directly toward the interface. It is apparent that since the σ phase actually grew much faster than this the growth must be aided by some other means.

One possibility is that growth is aided by the high concentration of Cu which is near the cluster when the phase nucleates. This region would provide plenty of solute for initial growth of the cube. In addition, as the σ phase grows, the volume strain of the cluster is relieved (since the atomic volume of σ is 12% less than that of the matrix), thereby releasing the vacancies to diffuse into the surrounding matrix. These vacancies could then aid in further diffusion of solute to the particle–matrix interface.

In addition to assistance from the Cu and vacancy-rich region near the initial cluster, growth of the σ phase may also be enhanced by dislocation diffusion. From Fig. 10 it can be seen that dislocations come in

contact with nearly all of the cubes. From micrographs of small (5–10 nm) cubes it was seen that σ does not actually nucleate on these dislocations. Instead, these dislocations seem to be attracted to the interface of a previously formed phase to help relieve the elastic strain, thus essentially becoming misfit dislocations. Diffusion along these dislocations would also help increase the rate at which solute arrives at the interface.

4.5. Nucleation of the θ′ phase

As mentioned earlier, the presence of the θ′ phase in the Al–4.3Cu–2Mg composite matrix was quite surprising since this phase is not normally detected in alloys with a Cu:Mg ratio less than 4:1. θ′ was not detected in the monolithic alloy with this same composition (only S′ was observed) or in the monolithic alloy after adding 0.35 wt % Si (in which case S′ and θ phase formed). Therefore it is suspected that as a result of interfacial reactions with SiO_2, a sufficient amount of Mg was depleted from the composite matrix to push the alloy into the S′ and θ two-phase region, as shown from the Al–Cu–Mg phase diagram in Fig. 11 [52]. After all, for the concentration of Si to reach a level sufficient for nucleation of the σ phase (approximately 0.5 at %), as much as 1 at % Mg would go to the formation of oxide at the interface (depending on the type of oxide formed). Hence in the composite matrix, the θ′ phase may actually be part of the transition series to the equilibrium θ phase.

The θ′ phase is commonly preceded by GP zones and θ″ when aged at temperatures below the θ″ solvus (approximately 220 °C). Ageing above the θ″ solvus would result in a low concentration of coarse θ′ which would nucleate on dislocations. However, in the composite matrix, a high concentration of fine-scale θ′ nucleated directly from the matrix during the rapid water quench as shown in Fig. 12. Many past studies have shown that a much denser distribution of θ′ can be achieved in Al–Cu alloys by work-hardening prior to ageing. The numerous dislocations provide many sites for direct nucleation of the θ′ phase, thus making formation of GP zones and θ″ unnecessary. It is also well known that a high dislocation density is produced in a composite material as it is cooled, due to differences in thermal expansion coefficients between the matrix and the reinforcement [53]. Consequently, the metastable θ′ phase was initially postulated to form during cooling of the composite by nucleating on these dislocations.

Evidence was later found which disputed this theory. When composite samples with small amounts of Si were air-cooled or quenched, a high concentration of θ′ had rapidly nucleated in many of them. However, when a composite with an Al–5Cu matrix (and thus no Si) was air-cooled or quenched, no θ′ nucleated; the Cu instead remained in solution. This observation suggested that Si was responsible for rapid nucleation of the θ′ phase, since both materials were composites with many dislocations available for nucleation. Furthermore, it can be seen from Fig. 10 that dislocations do not appear to interact with many

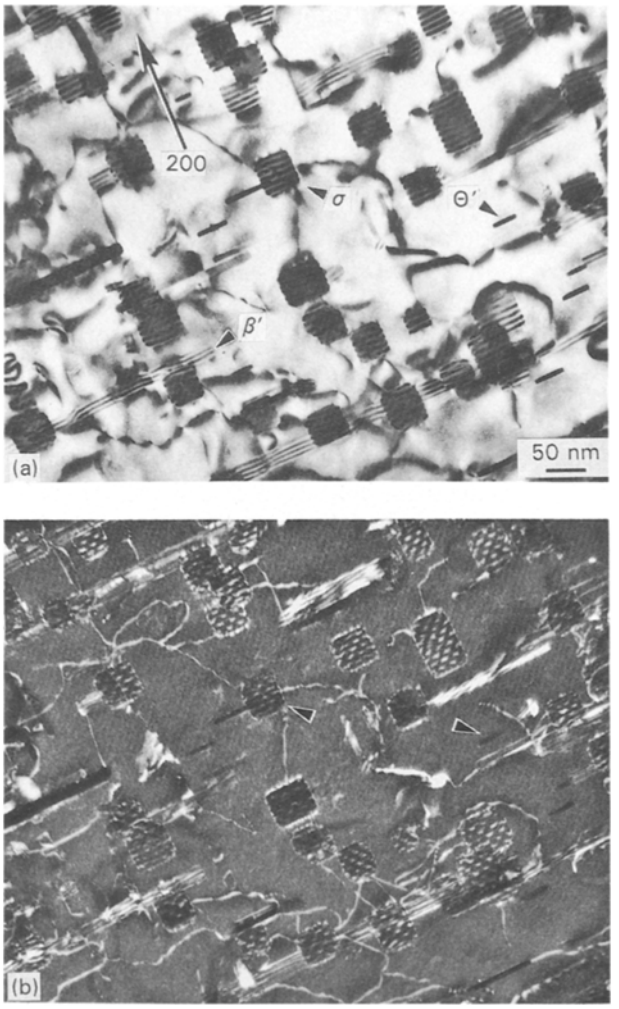

Figure 10 (A) Bright field and (b) WBDF with large + *s*. Dislocations are attracted to the σ interface.

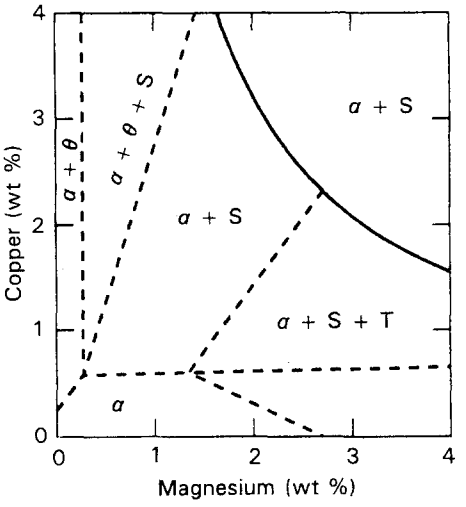

Figure 11 Aluminium-rich end of the Al–Cu–Mg phase diagram [52]: (——) phase boundaries at 500 °C, (– – –) possible phase boundaries at 190 °C.

of the small θ′ plates. suggesting that these phases did not nucleate on dislocations.

It is therefore proposed that θ′ nucleated from the Si (or Mg–Si) clusters in a manner similar to that described for the σ phase. If the concentration of Mg near the cluster was insufficient for nucleation of the σ

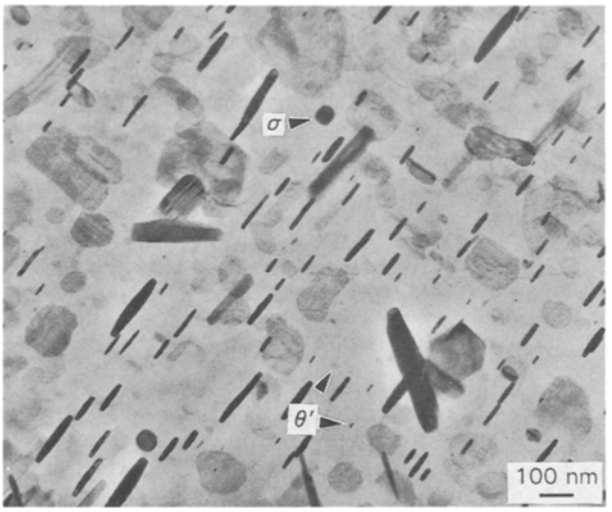

Figure 12 Al–4.3Cu–2Mg/Saffil composite as quenched. Small θ′ nucleates directly from the matrix.

phase, θ′ would instead be expected to nucleate in this high-Cu region. Since the atomic volume in θ′ is 4% less than that of Al, this compressed region would also offer reduced volume strain. This argument is supported by the fact that θ′ rarely nucleated along with the σ phase in the higher-Mg composite matrices (3–4 wt % Mg).

4.6. Nucleation in other systems

The nucleation mechanism proposed here for the σ and θ′ phases may also further our understanding of nucleation behaviour in other systems. For example, this same nucleation mechanism can be used to explain past studies which showed that additions of trace elements such as Cd, Sn and In to Al–Cu alloys resulted in rapid nucleation of the θ′ phase [6–10]. Binary phase diagrams [54] show that these elements, like Si, would also be driven out of solution during cooling to form clusters. In addition, Table I shows that clustering of these elements would create a compressive volume strain in the matrix, thus attracting Cu. This explanation agrees with the findings of previous investigators who have determined that fine-scale In, Sn and Cd precipitates rapidly nucleate during the early stages of ageing at 200 °C [55–57]. Upon further ageing these precipitates were shown to act as heterogeneous nucleation sites for the θ′ phase.

In addition, Brook and Hatt [46] have determined that when trace additions of Mg and Ge were added to an Al–Cu alloy, the Mg–Ge clusters which form nucleate the θ′ phase very efficiently; more so than Sn, In, Cd, Mg + Si or Si (with decreasing efficiency in that order). Ge is similar to Si in that it readily combines with Mg to form a high-enthalpy Mg_2Ge phase [58]. When an alloy containing Mg and Ge is quenched, Brook and Hatt have shown that small clusters of this phase form with vacancies being strongly bound to them. This suggests that a compressive stress is associated with the Mg–Ge clusters which may attract Cu atoms and nucleate θ′.

Furthermore, it was demonstrated by Auran *et al.* [12] that additions of Zn and Mg to an Al–Zr alloy significantly increased the nucleation rate of metastable Al_3Zr. Auran *et al.* believed that Al_3Zr nucleated from small η′ particles (Zn_2Mg) in the matrix. Although not enough is known about these phases to calculate the atomic volumes associated with them, Embury and Nicholson [59] have shown that formation of the Zn_2Mg phase is accompanied by an increase in atomic volume, thus suggesting that the atomic volume is greater than that of the aluminium matrix. In addition, these authors have shown that nucleation of this phase is highly dependent on vacancies. They suggest that vacancies may relieve the volume misfit strain, thus reducing the critical nucleus size. It is also known that Mg_2Si [12] and Si [60] can nucleate the Al_3Zr phase. Therefore it is proposed that the large atomic volume associated with these precipitates (Zn_2Mg, Mg_2Si, and Si) compresses the matrix and attracts the Zr atoms to their interface, resulting in nucleation of Al_3Zr.

Atomic volume differences may also be responsible for nucleation of the Ω phase by the combined addition of small amounts of silver and magnesium to Al–Cu alloys. The Ω phase was first observed in an Al–2.5Cu alloy after the addition of 0.5 wt % Mg and 0.5 wt % Ag [11]. This phase consists primarily of Al and Cu (in the ratio 2.6Al:1Cu [61]) and forms as plates which grow on the {1 1 1} aluminium planes. The structure of this phase has recently been shown to be orthorhombic with $a = 0.496$, $b = 0.859$ and $c = 0.848$ nm [62]. Muddle and Polmear [61] have established that precipitation of Ω results in a 9.3% reduction in average atomic volume, mostly due to a uniaxial contraction normal to the habit plane. These authors detected Ag at the interface of the Ω phase (Mg was also believed to accumulate at the interface but could not be detected due to limitations of the EDXS system). Taylor *et al.* [63] have speculated that Mg and Ag segregate to {1 1 1} planes and form small particles of hexagonal Mg_3Ag which serve to nucleate the Ω phase. Since the atomic volume in Mg_3Ag is 0.0201 nm^3 per atom this phase may attract Cu atoms and nucleate the Ω phase by the same mechanism proposed for θ′ and the σ phase. Note that this phase would also help to relieve the tensile stress which develops at the contracting interface of Ω after it has nucleated, thus explaining its presence at the interface. In this particular case the Cu atoms would accumulate on the {1 1 1} planes since Mg_3Ag forms on these planes. The resulting non-isotropic strain field could explain why Ω (an Al–Cu phase on {1 1 1} planes) nucleated rather than θ′ (an Al–Cu phase on {1 0 0} planes).

From the nucleation theory presented earlier, it would appear that additions of Cd, In, Sn or Ge may also nucleate the σ phase if added to Al–Cu–Mg alloys which are sufficiently high in Mg (1–2 wt %). These elements may provide a better nucleation site for the σ phase based on their larger atomic volume than Si (Table I) and their effectiveness at nucleating θ′. In addition, these elements are not known to exhibit the same segregation problems as Si.

5. Conclusions

The typical microstructure of a T7 heat-treated Al–4.3Cu–2Mg alloy was shown to contain vacancy loops with S′ nucleating on them, as expected. When this same alloy was squeeze-cast into an SiC preform and given an identical T7 heat treatment, the microstructure was found to contain S′, θ′, β′ and the unusual cubic σ phase.

The σ phase, along with θ′ and β′, were determined to nucleate rapidly in the composite matrix during the water quench following solution treatment (and not during artificial ageing). In Al–Cu–Mg alloys without Si, no precipitation took place during this quench. The S′ phase, on the other hand, nucleated more slowly during artificial ageing. For thin samples (< 2 mm thick) an effective method of forming the cubic σ phase is to quench directly to ageing temperatures between 240 and 340 °C.

The σ, θ′ and β′ phases were determined to nucleate as a result of excess Si in the composite matrix. This Si originated from breakdown of a SiO_2 layer on the interface of Si-containing whiskers. Mg in the alloy reacted with this silica layer during squeeze-casting, thus allowing free Si to diffuse into the matrix.

The Si is believed to nucleate the σ phase by a rather unconventional mechanism. Clusters of Si (or Mg_2Si) rapidly nucleate upon quenching and create a compressive volume strain in the matrix. This volume strain attracts a high concentration of vacancies and small Cu atoms to the interfacial region and thus provides an excellent atmosphere for nucleation of the σ phase. The θ′ phase is also believed to nucleate from these clusters in the event that insufficient Mg is available for σ phase formation.

In order for this σ phase to be useful, however, small cubes must be formed uniformly throughout the alloy, thus requiring a high nucleation rate. This has not yet been accomplished with the Si additions, mainly due to segregation effects. The addition of other elements (such as Cd, In, Sn or Ge) may therefore be required to obtain the necessary nucleation rate.

Acknowledgement

The authors would like to extend their appreciation to General Motors Corporation for supporting this project and for fabricating the composites studied.

References

1. R. D. SCHUELLER, A. K. SACHDEV and F. E. WAWNER, *Scripta Metall.* **27** (1992) 617.
2. *Idem, J. Mater. Sci.* **28** (1993) in press.
3. G. C. WEATHERLY, PhD thesis, University of Cambridge (1966).
4. R. N. WILSON, D. M. MOORE and P. J. E. FORSYTH, *J. Inst. Metals* **95** (1967) 177.
5. H. SUZUKI, I. ARAKI, M. KANNO and K. ITOI, *Trans. Jpn Inst. Light Met.* **27** (5) (1977) 239.
6. J. B. M. NUYTEN, *Acta Metall.* **15** (1967) 1765.
7. A. H. SULLY, H. K. HARDY and T.J. HEAL, *J. Inst. Met.* **76** (1949) 269.
8. H. K. HARDY, *ibid.* **78** (1950–51) 169.
9. R. SANKARAN and C. LAIRD, *Mater. Sci. Engng*, **14** (1974) 271.
10. W. X. FENG, F. S. LIN and E. A. STARKE Jr, in "Aluminum–Lithium Alloys II", edited by E. A. Starke, Jr and T. H. Sanders Jr (TMS–AIME, Warrendale, PA, 1983) p. 235.
11. J. H. AULD and J. T. VIETZ, in "The Mechanism of Phase Transformations in Crystalline Solids", Monograph No. 33 (Institute of Metals, London, 1969) p. 77.
12. L. AURAN, H. WESTENGEN and O. REISO, in Proceedings of 1st Riso International Symposium on Metallurgy and Materials Science, edited by N. Hansen, A. Jones, T. Leffers, Riso National Laboratory, Roskilde, Denmark (1980) p. 526.
13. L. F. MONDOLFO, "Aluminum Alloys: Structure and Properties" (Butterworth, London-Boston, 1976) p. 502.
14. R. N. WILSON and P. G. PARTRIDGE, *Acta Metall.* **13** (1965) 1321.
15. R. M. AKIN, Jr, NASA Contract Report 4365 (1991) p. 55.
16. R. N. WILSON, *J. Inst. Met.* **97** (1969) 80.
17. B. R. HENRIKSEN, *Composites* **21** (1990) 333.
18. S. L. MARR and F. K. KO, *Ceram. Eng. Sci. Proc.* **11** (1990) 1554.
19. H. J. HEGGE, J. BOETJE and J. M. DeHOSSON, *J. Mater. Sci.* **25** (1990) 2335.
20. C. H. LI, L. NYBORG, S. BENGTSON, R. WARREN and I. OLEFJORD, in Proceedings, "Interfacial Phenomena in Composite Materials '89", edited by F. R. Jones (Butterworth, Guildford, 1989) p. 253.
21. A. MUNITZ, M. METZGER and R. MEHRABIAN, *Met. Trans. A* **10A** (1979) 1491.
22. C. G. LEVI, G. J. ABBASCHIAN and R. MEHRABIAN, *ibid.* **9A** (1978) 697.
23. "Metals Handbook," 8th Edn, Vol. 8 (ASM, Metals Park, Ohio, 1973) p. 386.
24. L. F. MONDOLFO, "Aluminum Alloys: Structure and Properties (Butterworth, London-Boston, 1976) p. 499.
25. K. C. RUSSELL, "Phase Transformations" (ASM, Metals Park, Ohio, 1970) p. 291.
26. A. J. PERRY and K. M. ENTWISTLE, *J. Inst. Met.* **96** (1968) 344.
27. J. BURKE and A. D. KING, *Phil. Mag.* **21** (1970) 7.
28. A. J. PERRY and K. M. ENTWISTLE, *J. Inst. Met.* **96** (1968) 344.
29. J. TAKAMURA, K. OKAZAKI and I. G. GREENFIELD, *J. Phys. Soc. Jpn* **18** (1963) 78.
30. J. TAKAMURA, M. KOIKE and K. FURUKAWA, *J. Nucl. Mater.* **69/70** (1978) 738.
31. L. F. MONDOLFO, "Aluminum Alloys: Structure and Properties" (Butterworth, London-Boston, 1976) p. 369.
32. H. J. RACH and R. W. KRENZER, *Met. Trans. A* **8A** (1977) 335.
33. H. S. ROSENBAUM and D. TURNBULL, *Acta Metall.* **6** (1958) 653.
34. I. DUTTA and S. M. ALLEN, *J. Mater. Sci. Lett.* **10** (1991) 323.
35. I. KOVACS, J. LENDVAI and E. NAGY, *Acta Metall.* **20** (1972) 975.
36. M. F. ASHBY and G. C. SMITH *J. Inst. Met.* **91** (1962–63) 182.
37. A. T. STEWART and J. W. MARTIN, *ibid.* **98** (1970) 62.
38. D. W. PASHLEY, J. W. RHODES and A. SENDOREK, *ibid.* **94** (1966) 41.
39. D. L. W. COLLINS, *ibid.* **86** (1957–58) 325.
40. D. K. CHATTERJEE and K. M. ENTWISTLE, *ibid.* **101** (1973) 53.
41. N. E. FINK, *Acta Metall.* **7** (1959) 228.
42. E. OZAWA and H. KIMURA, *Mater. Sci. Engng*, **8** (1971) 327.
43. R. GEFFKEN and E. MILLER, *Trans. TMS–AIME* **242** (1968) 2323.
44. D. W. PASHLEY, M. H. JACOBS and J. T. VIETZ, *Phil. Mag.* **16** (1967) 51.
45. L. F. MONDOLFO, "Aluminum Alloys: Structure and Properties" (Butterworth, London-Boston, 1976) p. 568.
46. G. B. BROOK and B. A. HATT, in "The Mechanism of Phase Transformations in Crystalline Solids", Monograph No. 33 (Institute of Metals, London, 1967) p. 82.
47. J. T. VIETZ and I. J. POLMEAR, *J. Inst. Met.* **94** (1966) 410.
48. J. A. IBERS, *Acta Crystallogr.* **10** (1957) 86.

49. V. A. PHILLIPS and J. D. LIVINGSTON, *Phil. Mag.* **7** (1962) 969.
50. M. F. ASHBY and L. M. BROWN, *ibid.* **8** (1963) 1083.
51. N. L. PETERSON and S. J. ROTHMAN, *Phys. Rev. B* **1** (1970) 3264.
52. J. M. SILCOCK and B. A. PARSONS, Report R 10/67 (Fulmer Research Institute, 1958).
53. M. VOGELSANG, R. J. ARSENAULT and R. FISHER, *Met. Trans.* **17A** (1986) 379.
54. "Metals Handbook", 8th Edn, Vol. 8 (ASM, Metals Park, Ohio, 1973) pp. 258, 261, 263.
55. H. SUZUKI, M. KANNO and K. FUKUNAGA, *J. Jpn. Inst. Light Met.* **25** (1975) 413.
56. H. SUZUKI, M. KANNO and O. KANOH, *ibid.* **29** (1979) 223.
57. A. K. MUKHOPADHYAY, G. J. SHIFLET and E. A. STARKE Jr., in Proceedings of Morris E. Fine Symposium, edited by P. K. Liaw, J. R. Weertman, H. L. Marcus and J. S. Santner (TMS, Warrendale, PA, 1991) p. 283.
58. A. LUTTS, *Acta Metall.* **9** (1961) 577.
59. J. D. EMBURY and R. B. NICHOLSON, *ibid.* **13** (1965) 403.
60. O. REISO, H. WESTENGEN, L. AURAN and ARDAL OG SUNNDAL VERK, Sunndaisora (Norway).
61. B. C. MUDDLE and I. J. POLMEAR, *Acta Metall.* **37** (1989) 777.
62. K. M. KNOWLES and W. M. STOBBS, *Act. Crystallogr.* **B44** (1988) 207.
63. J. A. TAYLOR, B. A. PARKER and I. J. POLMEAR, *Met. Sci.* **20** (1978) 478.

Received 2 February
and accepted 29 June 1993